

NRC Publications Archive Archives des publications du CNRC

Textured panel for ice-induced vibration mitigation and reduction of associated average load

Gagnon, Robert E.

This publication could be one of several versions: author's original, accepted manuscript or the publisher's version. /
La version de cette publication peut être l'une des suivantes : la version prépublication de l'auteur, la version acceptée du manuscrit ou la version de l'éditeur.

Publisher's version / Version de l'éditeur:

Proceedings of the 28th International Conference on Port and Ocean Engineering under Arctic Conditions (POAC'25), pp. 1-11, 2025-08

NRC Publications Archive Record / Notice des Archives des publications du CNRC :

<https://nrc-publications.canada.ca/eng/view/object/?id=a6b76d64-26e4-40c8-9a80-d0645d54a8b1>
<https://publications-cnrc.canada.ca/fra/voir/objet/?id=a6b76d64-26e4-40c8-9a80-d0645d54a8b2>

Access and use of this website and the material on it are subject to the Terms and Conditions set forth at
<https://nrc-publications.canada.ca/eng/copyright>

READ THESE TERMS AND CONDITIONS CAREFULLY BEFORE USING THIS WEBSITE.

L'accès à ce site Web et l'utilisation de son contenu sont assujettis aux conditions présentées dans le site

<https://publications-cnrc.canada.ca/fra/droits>

LISEZ CES CONDITIONS ATTENTIVEMENT AVANT D'UTILISER CE SITE WEB.

Questions? Contact the NRC Publications Archive team at
PublicationsArchive-ArchivesPublications@nrc-cnrc.gc.ca. If you wish to email the authors directly, please see the first page of the publication for their contact information.

Vous avez des questions? Nous pouvons vous aider. Pour communiquer directement avec un auteur, consultez la première page de la revue dans laquelle son article a été publié afin de trouver ses coordonnées. Si vous n'arrivez pas à les repérer, communiquez avec nous à PublicationsArchive-ArchivesPublications@nrc-cnrc.gc.ca.



POAC'25
St. John's,
Newfoundland and
Labrador, Canada

Proceedings of the 28th International Conference on
Port and Ocean Engineering under Arctic Conditions
Jul 13-17, 2025
St. John's, Newfoundland and Labrador
Canada

Textured Panel for Ice-Induced Vibration Mitigation and Reduction of Associated Average Load

Robert E. Gagnon
National Research Council Canada, St. John's, Canada

ABSTRACT

Based on understandings of the mechanisms that constitute ice-spallation phenomena, gleaned from various ice-crushing lab tests conducted at NRC, it was determined that it should be possible to incorporate low-profile textural patterns/components into the design of a structure's faces that could disrupt the spalling process. This was confirmed in earlier small-scale lab tests that showed that during ice crushing when using NRC's Blade Runners technology (Patent US 9,181,670 B2), instead of a series of large-amplitude spallation-induced sawtooth load spikes, a considerably greater number of much smaller ice spallations, and associated load-spikes, were produced due to the textured surface's ability to initiate spallation. While the average load in that case basically remained the same with or without the surface technology, the amplitude of the sawteeth load spikes was greatly reduced. Consequently, due to the invariance of ice properties in the brittle regime over a wide range of scale, the Blade Runners technology has the potential capability to reduce the amplitude of the sawtooth load pattern that develops due to repetitive ice spallations that occur when a moving ice sheet crushes against an offshore platform, such as a wind turbine or oil/environmental-monitoring platform. Here, we present a new technology that uses an essential aspect of the physics underlying the earlier Blade Runners technology, i.e., spallation initiation/disruption, but uses it in a manner requiring less surface modification than the former technology stipulates, to not only reduce the amplitude of the spallation-induced sawtooth load pattern, but also to reduce the average ice load. Data from lab tests using the new technology are discussed.

KEY WORDS: Ice-induced vibration mitigation; Ice load reduction; Ice-sheet-edge spallation disruption.

INTRODUCTION

Ice crushing induced vibration, associated with ice sheets encroaching on offshore structures, has been a subject of interest for several decades. The most widely known and studied events are those associated with the Gulf Canada Resources Ltd. Molikpaq caisson facility that occurred in 1986 during operations at the Amauligak I-65 site in the Canadian Beaufort Sea (e.g., Jefferies, 2010). Various analytical and numerical approaches (e.g., Karna et al., 1999; Hendrikse and Nord, 2019; and Gagnon 2022) have been applied to explain ice crushing induced vibration. Some of this work was focused on new understandings of ice crushing, with emphasis on spalling behavior, where the main behaviors observed during the Molikpaq incidents were successfully reproduced in numerical simulations (Gagnon, 2022). Furthermore, a new technology known as Blade Runners (Patent US 9,181,670 B2) was introduced and tested at lab-scale, involving disruption of the ice-spallation process, that significantly reduced the amplitude of the sawtooth load patterns that cause ice-induced vibration, though not affecting the average ice load. Here we present lab-test results of a more recent related technology, with similar ice-spallation disruption capability as Blade Runners, and potential added benefits of reducing the average ice load during ice-sheet encroachment events while requiring less modification to the ice-facing structure surface.

BRIEF REVIEW OF ICE CRUSHING MECHANISMS IN THE BRITTLE REGIME

Here we provide a brief review of ice crushing characteristics in the brittle regime. Many studies (e.g., Gagnon, 1999; Riska et al., 1990; Fransson et al., 1991) have shown that during the crushing there are regions of relatively intact ice (hard zones), small compared to the nominal contact area, in the contact zone that are surrounded by crushed ice which extrudes/flows away from the intact zones. The peripheral crushed ice is essentially the debris of shattered spalls that have previously broken away sequentially from the intact hard zone, where the spallation sequence has a one-to-one association with the sequence of sharp load drops in the classic sawtooth load pattern that is generated. Microcracking may be present in a hard-zone region of the ice during crushing/indentation, however hard zones have been observed to maintain significant load bearing capacity and sustain high pressures (as though fully intact) even when microcracks are present (Gagnon and Bugden, 2007). Hence, we often use the term ‘relatively intact ice’. Due to the compliance of the ice/apparatus system, during continuous crushing the actual penetration of the ice has a degree of intermittency that directly correlates with the sawtooth load pattern.

Various studies have shown that ice crushing, at least at rates in the brittle regime, is highly geometrical (e.g., Daley, 1991; Evans et al., 1984; Gagnon, 1999; Spencer and Masterson, 1993). That is, spalling events are determined for the most part by the geometry of the ice formation and the depth of penetration, where both can influence the level of confinement. For example, if a platen crushes a pyramid-shaped ice formation at a fixed rate, the frequency of the spalling will be higher for a given penetration if the pyramid has steeper sides because in that case there is less confinement of the ice in the contact zone and spall-initiating fractures can occur at generally lower loads and less strain in the ice-apparatus system. Hence, for a given displacement of the platen more spalls occur when the pyramid has steeper sides. Furthermore, as the penetration depth increases in either case of the two different pyramids the level of confinement increases and the spalling frequency decreases. In the case of crushing at the edge of an ice sheet the geometry of the ice crushing process surface does not alter as crushing proceeds since confinement of the ice associated with the sheet’s thickness is constant,

and we can therefore expect spallations at regular intervals of penetration. If the rate of penetration varies, then the spalling frequency varies accordingly since each spall is associated with a certain amount of penetration. The Molikpaq data, associated with various ice sheets crushing against it, show the spalling rate dependence on ice sheet speed (Gagnon, 2012). Furthermore, the crushing of ice pyramids in the lab also shows the spalling rate dependence on actuator speed/crushing rate (Gagnon, 1994). The same type of spalling rate dependence on actuator speed was noted for the Ice Island experiments (Kennedy et al., 1994), and for crushing experiments using wedge-shaped ice specimens in the lab (Tukhuri, 1995).

Another important aspect of ice crushing in the brittle regime is that for any sawtooth in the sawtooth load pattern generated during ice crushing, ice is removed from the structure/ice-hard-zone interface by the erosive action of a thin slurry-layer mix of tiny ice particles and liquid (Gagnon, 2016). This happens rapidly during the load drop portion of the sawtooth, and much more slowly on the ascending portion.

EXPERIMENTAL SETUP AND RESULTS FROM THE LAB TESTS

The essentials of the new technology are described in Figures 1 and 2 that show an acrylic ice-crushing platen that has an inscribed square pattern of small linear ridges that each have a triangular section profile. The ridges are 0.25 mm in height and have a base that is 1.0 mm wide. The spacing between the base edges of adjacent ridges is 1.0 mm. Accordingly, the spacing between the tops of adjacent ridges is 2.0 mm. The inscribed platen surface is divided into two regions, one where the ridges are horizontal, and one where they are vertical. Each vertically-oriented ridge intersects with a horizontally-oriented ridge at some point along the diagonal of the square inscribed pattern.

The technology works by utilizing two principles. One principle is the initiation of many relatively-small spallations, due to the ridges on the textured surface of the platen that serve as spall nucleators. A platen without ridges, on the other hand, would result in significantly fewer, but much larger spallations, that generate a typical high-amplitude sawtooth load pattern associated with ice crushing. In the same way that the Blade Runners technology functions by reducing the amplitude of the typical sawtooth load patterns during ice crushing in the brittle regime, the new technology achieves the same result, but with a much lower section profile of the ridges than the former technology prescribes in its patent claims. In addition to the reduction of the sawtooth load pattern amplitude, the new technology also generates a non-uniform asymmetric stress field in the bulk ice that further increases the likelihood of fracture and the nucleation of spalls. The additional reduction of the average load that is evident

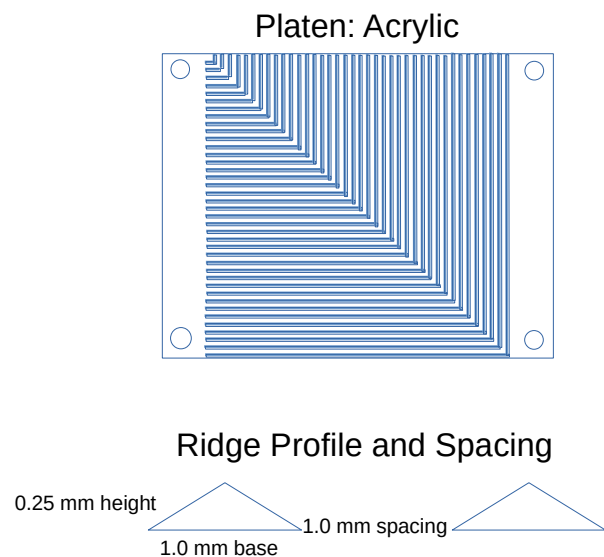


Figure 1. Top-view schematic of the acrylic textured-surface ice-crushing platen. The low-profile triangular ridges are the sets of vertical and horizontal lines that intersect at the diagonal of the square textured region of the platen's surface.

using the new technology, which does not happen using the Blade Runners technology, is attributed to the non-uniform asymmetric stress field associated with the unique pattern of the ridges as shown in Figures 1 and 2.

The non-uniform asymmetric stress field arises because the linear ridges tend to cause spallation in the lateral directions normal to the ridges. The bulk ice sample crushes against the platen and is approximately centered on the diagonal line that separates horizontal ridges from vertical ridges. Hence, on average, half of the hard-zone ice contacting the platen is experiencing forces from the vertical ridges that generate spallation generally to the left and right (with respect to Figure 1), while the other half of the hard-zone ice is experiencing forces from the horizontal ridges that cause spallation in the upwards and downwards directions. This situation creates an asymmetric stress field in the ice that increases its susceptibility to fracture, thereby further reducing its load-bearing capacity. That is, the average load is also reduced. Another contributing factor to the asymmetric stress field is the flow direction of the pressurized crushed ice (shattered spall debris) generated by the spallations. The crushed ice tends to flow along the ridge directions. Hence, asymmetric lateral forces may be produced in the bulk ice sample due to the pressurized crushed-ice material interaction arising from the differing flow directions associated with the vertical and horizontal ridges.

An extensive series of ice-crushing experiments were conducted using the platen depicted in Figures 1 and 2, and other platens with differing variations of the inscribed pattern. A platen with no ridges on its surface was also used to establish a base-line from which the effectiveness of the differing textured platens could be determined. The ice samples were obtained from larger blocks of polycrystalline freshwater ice grown in the lab. The ice samples had a square-column shape with a truncated-pyramid top (Figure 3). The dimensions of the samples were approximately 7.0 cm x 7.0 cm x 7.0 cm, and the slopes on the truncated pyramid-shaped tops were about 40° to horizontal. The grain size of the ice was approximately 4 mm in diameter.

Figure 4 shows the time-series load records for two typical ice-crushing experiments, one using a flat crushing platen and the other using the best-performing textured-surface platen (shown in Figures 1 and 2). The ice specimens were crushed at a rate of 16 mm/s to a depth of approximately 35 mm. The ambient temperature for all tests was -10 °C. The classic

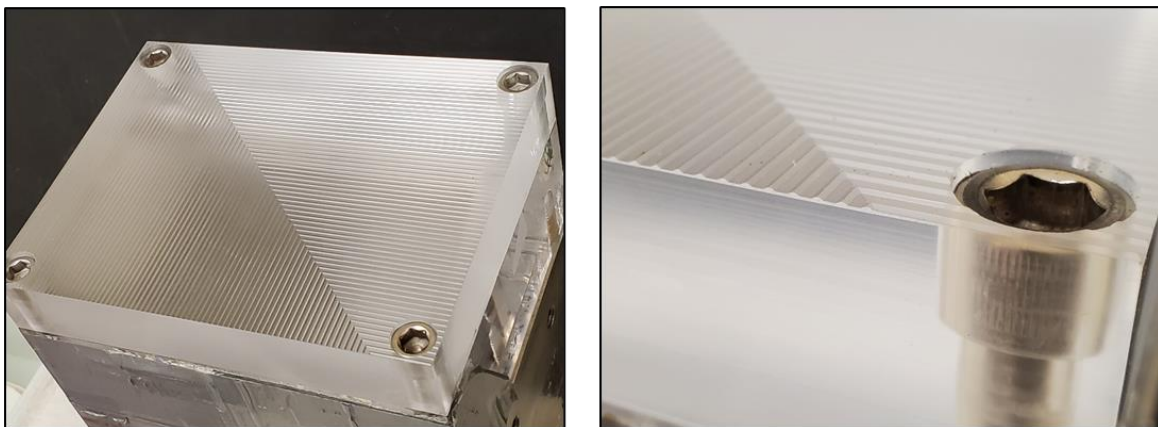


Figure 2. Photographs of the acrylic textured-surface ice-crushing platen illustrated in Figure 1: (Left) Full view of the platen top; (Right) Expanded view of one corner of the platen where details of the small linear ridges may be discerned.

high-amplitude sawtooth load pattern for ice-crushing in the brittle regime is prominent in the load record for the flat platen. Equally striking is the much smoother load record for the textured-surface platen, which features a relative lack of high-amplitude load sawteeth. These features are further illustrated in the frequency-domain plots of the two load records (Figure 5). Another important aspect of the load data is that the average local-time value of the load for the textured-surface platen, throughout the major portion of the tests, is lower than the corresponding value for the flat platen. These features are due to both the spall-initiation capability of the small ridges on the textured-surface platen and the pattern of the ridges, as discussed above.

Since data from ice crushing experiments in the brittle regime typically exhibits considerable scatter, it is always necessary to conduct at least three experiments for any set of parameters to establish statistical reliability for comparative analysis. To investigate the efficacy of the textured-surface platens that were

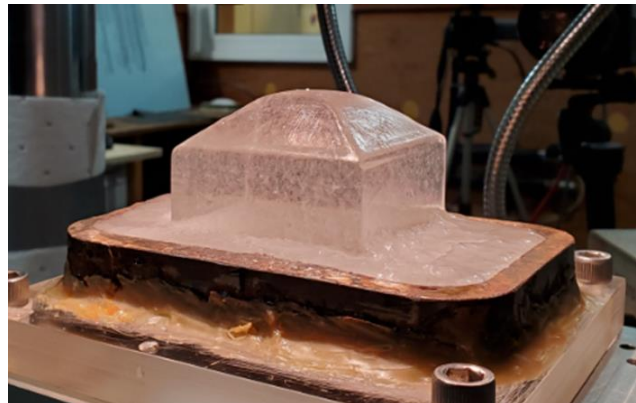


Figure 3. Photograph of a polycrystalline freshwater ice specimen prior to an ice-crushing test. The ice sample had a square-column shape with a truncated-pyramid top. It was frozen into a metal/acrylic ice-holder by freezing a layer of water-saturated snow around its base. The acrylic base-plate of the holder is visible at the bottom. A thick steel confining perimeter, attached to the base-plate, contains the frozen snow and ice sample.

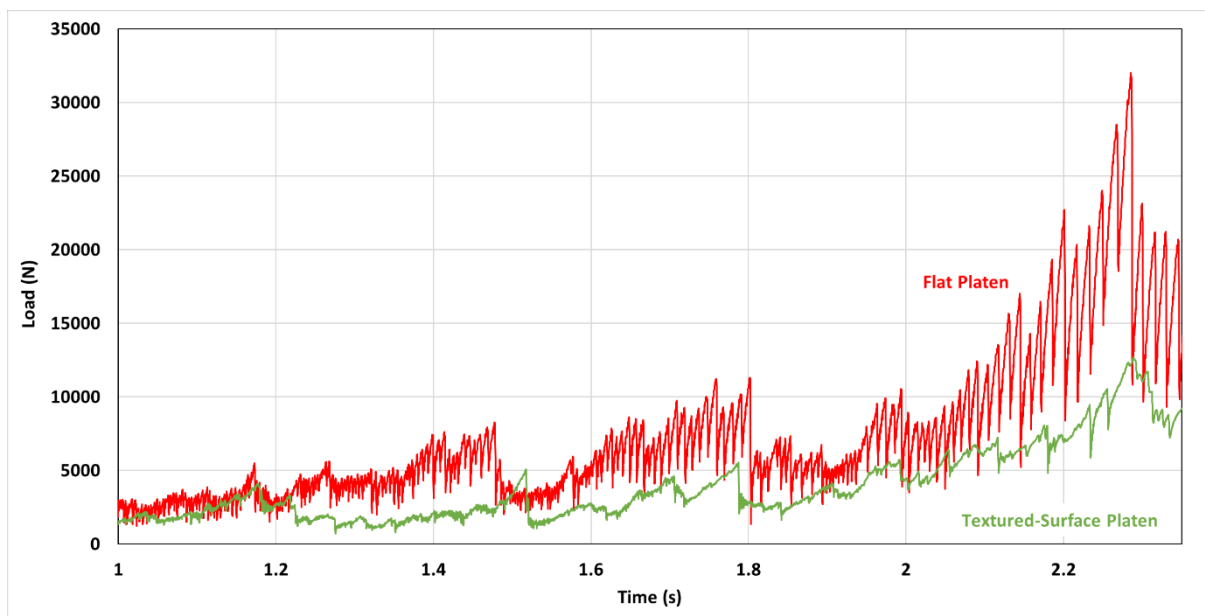


Figure 4. The major portions of typical time-series load records for two ice-crushing tests, one (red plot) utilizing the smooth flat platen and the other (green plot) using the best-performing textured-surface platen.

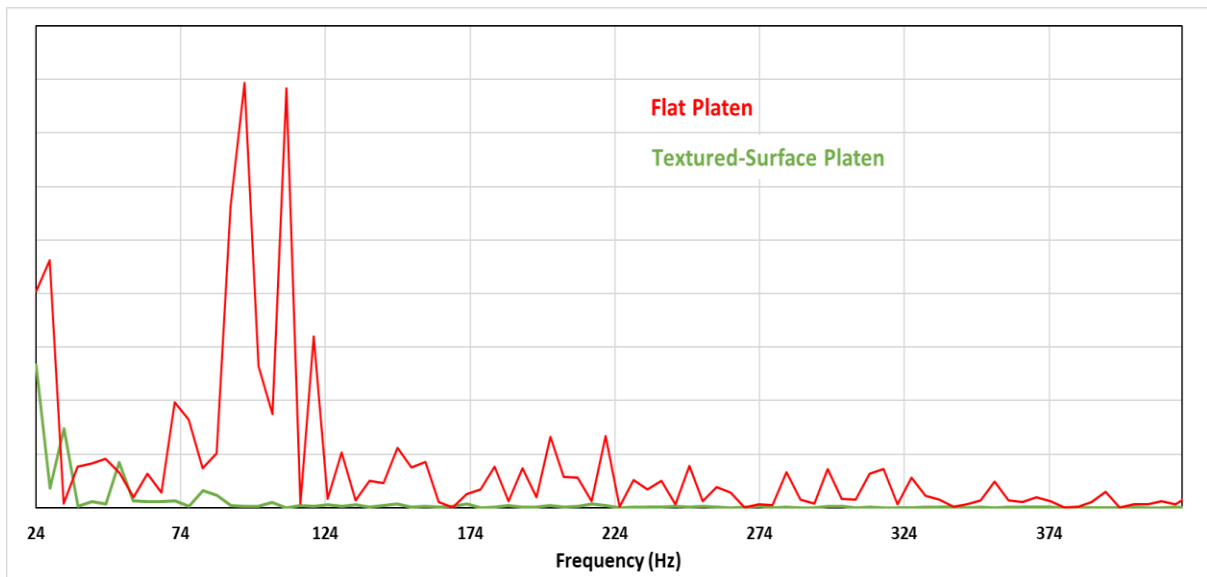


Figure 5. Frequency-domain (FFT) plots for the two tests shown in Figure 4.

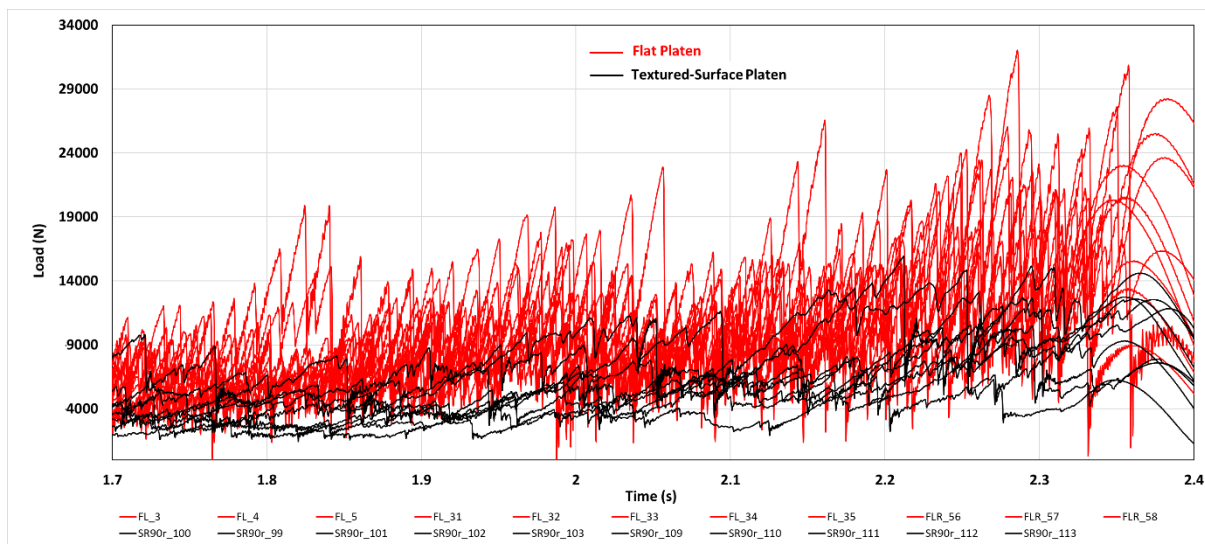


Figure 6. The major portions of the time-series load records from twenty-one ice-crushing tests, eleven (red plots) utilizing the smooth flat platen and the other ten (black plots) using the best-performing textured-surface platen.

fabricated, at least five experiments have been performed in each case, and more typically five to eleven experiments for the platens showing the most promise. Figure 6 shows a portion of the time-series load data for eleven ice-crushing tests using the flat platen and ten tests using the textured-surface platen shown in Figures 1 and 2. In spite of the congestion of data points the information presented is essentially the same as was evident in Figure 4, but now with statistical significance. As an aid to appreciate more easily what was presented in Figure 6, we have plotted in Figure 7 only the maximal value of the load for each set of experiments at each instant in time. For example, at time 2.2 s, only the highest load value from the set of eleven values from the flat-platen tests was plotted. The ten experiments using the textured platen were separated into two sets of five, to illustrate the similarity of results even when the test sets were conducted on different days during the test program, and where ice samples were cut from

differing areas of the parent ice block or different blocks. As before, only the highest load value from the set of five values for the textured-surface platen tests was plotted at each time instant. Since the sawtooth load peaks for the flat platen are closely spaced, we have roughly traced the peak tops as an aid in comparing the three data plots. The data trends and conclusions one can make from Figure 4 are basically the same as what one could surmise from the much more statistically significant plots in Figure 7.

Note that in this test program four different surface-texture patterns and two textured-pattern profile heights were tested/evaluated. A textured-surface pattern variation of that in Figures 1 and 2, where the pattern of ridges intersected at 45° , was found to be ineffective at reducing loads when the profile height was 0.5 mm, whereas some load-reduction effect was evident when the profile height was 0.25 mm. It was deemed a reasonable assumption that a similar effect would apply to the case where the pattern of ridges intersected at 90° . As has been previously stated, the best-performing textured platen was that shown in Figures 1 and 2, where the linear ridges were 0.25 mm in height and they intersected at a 90° angle. Another set of experiments using this platen, where the platen itself was rotated 45° to its former orientation with a side edge of the ice aligned with the long axis of the platen, showed no effect associated with the rotation. When ice was crushed against ridges oriented in one direction there was no definitive reduction of average load or sawtooth amplitude.

The application of the technology to reduce ice-induced vibration (IIV) and average ice loads on an offshore structure, may have several possible configurations. As already pointed out, the technology appears to function optimally when the anticipated loads of concern to a structure match the size of the fundamental pattern. That is, the 'unit' textured-patch size would be a symmetric square area as in the schematic in Figure 1. In the present crushing tests, a portion

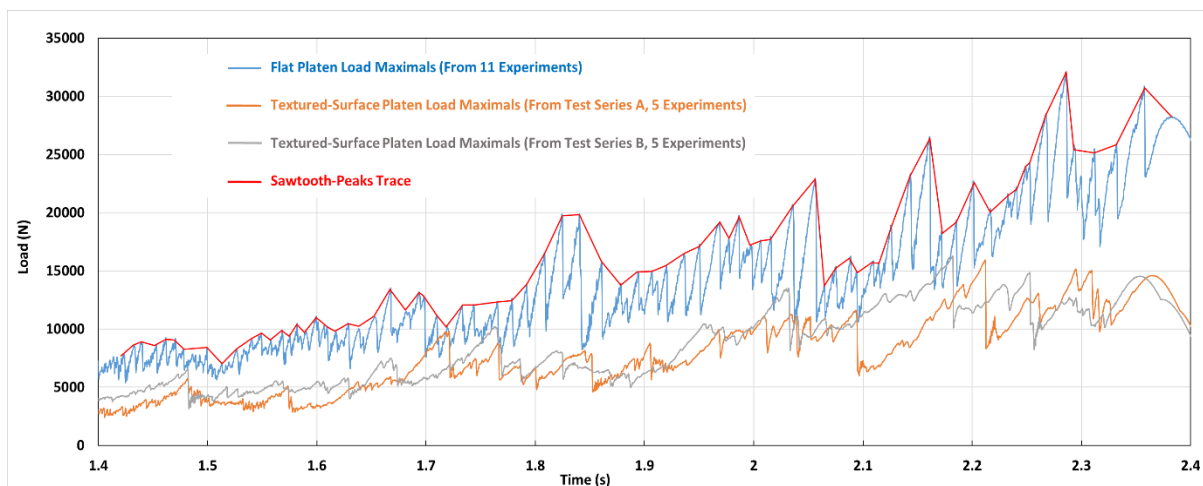


Figure 7. The major portions of the time-series maximal-load values for the eleven ice-crushing experiments conducted using the smooth flat platen (blue plot), and for the ten tests conducted using the best-performing textured-surface platen (orange and grey plots). The ten experiments using the textured platen were separated into two sets of five, to illustrate the similarity of results even when the test sets were conducted on different days during the test program, and where ice samples were cut from differing areas of the parent ice block or from different blocks. The maximal value of the load for each of the three sets of experiments is plotted at each instant in time. Since the sawtooth load peaks for the flat platen are closely spaced, we have roughly traced the peak tops as an aid in comparing the three data plots.

of that area was suitable to encompass the ice-crushing contact area associated with the maximal loads that were measured (~ 25 kN) using the smooth flat platen. Hence, since ice contact area and load are linearly related, the ‘unit’ textured-patch size on a structure’s surface where maximum anticipated loads are, for example, in the 0.5 MN range would scale according to a load ratio of 0.5 MN divided by 25 kN, which equals 20. This implies that all linear dimensions of the ‘unit’ textured-surface patch would increase by a factor equal to the square root of 20, i.e., 4.47. Since the used patch size during the ice crushing tests was basically the area of the section of the square-column ice sample (i.e., 7 cm x 7 cm) = 49 cm², we expect that for the full-scale case of a real structure the ‘unit’ textured-patch size should be about 20 x 49 cm² = 980 cm². This implies that the square-patch ‘unit’ area would have approximate dimensions 31 cm x 31 cm. Similarly, the dimensions of the triangular ridges’ base width, height and peak-to-peak spacing would be 4.47 mm, 1.12 mm and 8.94 mm respectively. This example is associated with freshwater ice (or low-salinity ice), such as forms in the Great Lakes, the Baltic and Bohai Seas (where the water is brackish), and multiyear sea ice in Arctic regions. It also relates to glacial ice masses that are sometimes embedded in multiyear sea ice sheets. In the case of sea ice sheet / structure interactions, the ice at the contact interface might be somewhat ‘softer’ than freshwater ice, if it is younger than multiyear ice, in which case the ridge heights might need to be marginally increased. Experiments with actual sea ice would be needed to investigate this.

Figures 8 and 9 show two of the possible configurations of groups of ‘unit’ textured areas as they might be on the face of an offshore structure. In each case one of the ‘unit’ textured areas is outlined in yellow.

For context, we now refer to an illustration (Figure 10) from the description of the former Blade-Runners technology as a reminder of what the origin of ice-induced vibration of a structure is, and more pertinent to the discussion here, to also show where placement of a suitable panel of the type described above would be on the structure’s face to mitigate IIV. If we ignore the orange feature for the moment, Figure 10 shows a train of large regular spallations, extending into the plane of view to the full width of the structure, that will occur

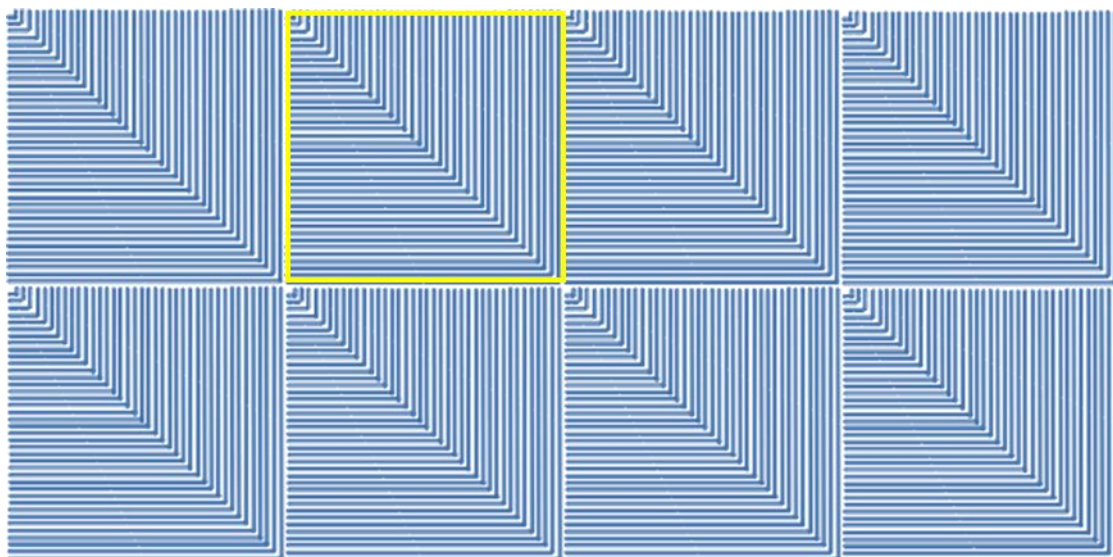


Figure 8. Configuration of a group of ‘unit’ textured areas where adjacent edges don’t match and the ‘unit’ diagonals are globally diagonal: scenario 1. One of the ‘unit’ textured areas is highlighted in yellow.

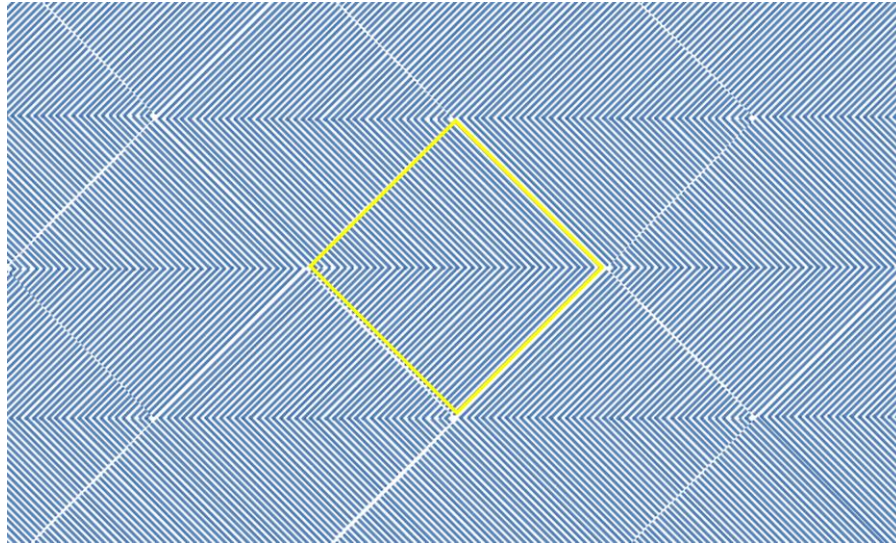


Figure 9. Configuration of a group of ‘unit’ textured areas where adjacent edges match and the ‘unit’ diagonals are globally horizontal: scenario 2. One of the ‘unit’ textured areas is highlighted in yellow.

as the ice sheet moves toward the left and crushes against the vertical face of the structure when no IIV mitigating panel is on its face. Note that a sequence of idealized spallations as in Fig. 10 may not represent the exact shapes of the spalls, which likely have some curvature to them, but the regularity and spacing/thickness (5.4 cm) have been well established for one of the 1986 ice-sheet encroachment events against the Molikpaq structure. Now considering that the orange

feature in the schematic is a panel of the type described above, we would expect that the regular train of large spallations will be disrupted, in time and space, so that many more, and much smaller, spallations occur in an unsynchronized manner across the structure’s face. The panel has to at least encompass the hard-zone region of the structure/ice contact zone to function with the greatest efficiency. In practical terms, the panel could be centered on the mid-height of the thickness of the ice sheet, and extend upwards and downwards to near, or slightly more than, the full thickness of the ice sheet. This ensures that the hard-zone is fully encompassed by the IIV mitigating technology, since the hard zone is known to stay quite localized in the mid region of the ice-sheet thickness, as has been shown in various real ice-edge crushing experiments (e.g., Frederking, 2004; Määttänen et al., 2011; Sodhi et al., 2001; Takeuchi et al., 1997).

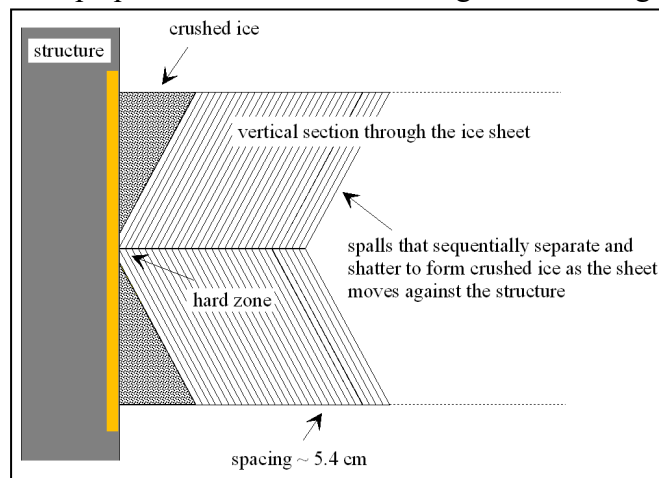


Figure 10. Schematic illustrating the sequence of spallations that will occur as an ice sheet moves to the left and crushes against the Molikpaq-type structure when no IIV mitigating technology is present. Regions of relatively soft crushed ice, located above and below a central region of relatively intact hard ice, are also indicated [from Gagnon (2012), with added orange feature]. The orange feature shows where an IIV mitigation panel could be placed that would radically disrupt the regular train of spallations in the beneficial manner described above.

CONCLUSIONS

Here we have shown results from small-scale ice-crushing experiments against a novel textured-surface panel which demonstrated significant reduction in amplitude of the characteristic sawtooth load pattern that occurs during ice crushing in the brittle regime. The test results also exhibited a substantial reduction in the average ice load. The ability to significantly enhance the nucleation of ice-spallation events, that is, create many more and much smaller events, while also imposing an asymmetric confinement regime on the bulk ice are the two mechanisms underlying the technology's facility to reduce both IIV and the average ice load, respectively. Due to the invariance of ice-crushing behavior over a wide range of scale in the brittle regime, we anticipate that this technology has potential for mitigation of IIV of offshore structures, which arises from ice-spallation-generated sawtooth load patterns, and average ice-load reduction. Here we used acrylic platens because they facilitate visual observation of the ice crushing behavior, while providing essentially the same results as the metal platens that were tested. For actual usage on offshore structures, steel or some other metal plating would likely be used, where textured plates could be installed by welding or bolting.

ACKNOWLEDGEMENTS

The author is grateful to the National Research Council Canada for its support of this work, and also acknowledges expressions of interest from industry. The expert technical assistance of Austin Bugden during the experiments was highly valued.

REFERENCES

- Daley, C.G., 1991. Ice edge contact and failure. *Cold Reg. Sci. Technol.* 21, 1–23.
- Evans, A.G., Palmer, A.C., Goodman, D.J., Ashby, M.F., Hutchison, J.W., Ponter, A.R.S., Williams, G.J., 1984. Indentation spalling of edge-loaded ice sheets. In: *Proceedings of IAHR 1984, Hamburg*, pp. 113–121.
- Fransson, L., Olofsson, T., Sandkvist, J., 1991. Observations of the failure process in ice blocks crushed by a flat indenter. *Proceedings of the 11th International Conference on Port and Ocean Engineering Under Arctic Conditions.* 1, pp. 501–514.
- Frederking, R., 2004. Ice Pressure Variations during Indentation. *Proc. IAHR Symposium on Ice, St. Petersburg, Russia*, pp. 307–314.
- Gagnon, R.E., 1994. Generation of melt during crushing experiments on freshwater ice. *Cold Reg. Sci. Technol.* 22 (4), 385–398.
- Gagnon, R.E., 1999. Consistent observations of ice crushing in laboratory tests and field experiments covering three orders of magnitude in scale. *Proceedings of POAC-99*, 2, pp. 858–869.
- Gagnon, R., 2012. An Explanation for the Molikpaq May 12, 1986 Event. *Cold Regions Science and Technology* 82 (2012) 75-93.
- Gagnon, R.E., 2015. Large scale spallation inducing ice protection. US Patent 9,181,670 B2,

Nov. 10, 2015.

Gagnon, R.E., 2016. New friction mechanisms revealed by ice crushing-friction tests on high-roughness surfaces. *Cold Reg. Sci. Technol.* 131 (2016), 1–9.

Gagnon, R., 2022. Spallation-based numerical simulations of ice-induced vibration of structures. *Cold Regions Science and Technology* 194 (2022) 103465.

Gagnon, R.E., Bugden, A., 2007. Ice crushing tests using a modified novel apparatus. POAC-07, Dalian, China, June 27-30, 2007.

Hendrikse, H., Nord, T.S., 2019. Dynamic response of an offshore structure interacting with an ice floe failing in crushing. *Mar. Struct.* 65 (2019), 271–290.

Jefferies, M., 2010. Molikpaq dynamic ice–structure interaction at Amauligak 1985–6: measurements and data. Ice Induced Vibrations JIP workshop 29th -30th of November, Oslo, Norway. Copies can be obtained from M. Jefferies at geomek@hotmail.com.

Karna, T., Kamesaki, K., Tsukuda, H., 1999. A numerical model for dynamic ice–structure interaction. *Comput. Struct.* 72, 645–658.

Kennedy, K.P., Jordaan, I.J., Maes, M.A., Prodanovic, A., 1994. Dynamic activity in medium-scale ice indentation tests. *Cold Reg. Sci. Technol.* 22 (3), 253–267.

Mänttänen, M., Marjavaara, P., Saarinen, S., 2011. Ice crushing pressure distribution against a compliant stiffened panel. Proc. 21st Int. Conf. On Port and Ocean Engineering under Arctic Conditions, Montreal, Canada, POAC 2011, paper #038.

Riska, K., Rantala, H., Joensuu, A., 1990. Full Scale Observations of Ship-ice Contact. Laboratory of Naval Architecture and Marine Engineering, Helsinki University of Technology (Report M-97).

Sodhi, D.S., Takeuchi, T., Nakazawa, N., Kawamura, S.A.M., 2001. Measurements of ice force and interfacial pressure during medium-scale indentation tests in Japan. Proc. 16th International Conference on Port and Ocean Engineering under Arctic Conditions, Ottawa, Ontario, Canada, pp. 617–626.

Spencer, P.A., Masterson, D.M., 1993. A geometrical model for pressure aspect-ratio effects in ice-structure interaction. *Proceedings of OMAE* 1993 (4), 113–117.

Takeuchi, T., Masaki, T., Akagawa, S., Kawamura, M., Nakazawa, N., Terashima, T., Honda, H., Saeki, H., Hirayama, K., 1997. Medium-scale field indentation tests (MSFIT)—ice failure characteristics in ice/structure interactions. Proc. of the 7th Int. Offshore and Polar Engineering Conference, Honolulu, USA, vol. II, pp. 376–382.

Tukhuri, J., 1995. Experimental observations of the brittle failure process of ice and ice structure contact. *Cold Reg. Sci. Technol.* 23 (1995), 265–278.